Direct Observation of Two Dimensional Magic Clusters

M. Y. Lai and Y. L. Wang*

Institute of Atomic and Molecular Sciences, Academia Sinica, P.O. Box 23-166, Taipei, Taiwan
and Department of Physics, National Taiwan University, Taipei, Taiwan

(Received 25 March 1998)

Two dimensional magic clusters have been directly observed on the $\sqrt{3} \times \sqrt{3}R30°$ reconstructed Ga/Si(111) surface using scanning tunneling microscopy. The magic numbers are $n(n + 1)/2$, where n (2, 3, 4, or 5) is the number of atoms on each side of these triangular clusters with preferred orientation with respect to the substrate. The $\sqrt{3} \times \sqrt{3}R30°$ adatom lattice surrounding the magic clusters exhibits characteristic vacancies. A structural model is proposed to account for the cluster orientation and lattice vacancies as well as the extraordinary abundance and stability of the decamers ($n = 4$). [S0031-9007(98)06520-X]

PACS numbers: 68.35.Bs, 61.16.Ch

Magic clusters, i.e., clusters with enhanced stability at certain sizes, have been intensively studied over the last decade. For magic clusters in free space, many interesting results about their electronic and atomic shell structures are found in the literature [1–6]. In contrast, magic clusters supported by a substrate (henceforth referred to as 2D magic clusters) are rarely discussed. Only recently have researchers found indirect evidence of such clusters in a molecular beam scattering experiment [7] and issues related to the stability of clusters on various substrates caught researchers' attention [8,9]. The main difference between free and supported clusters lies in the presence of the supporting substrate for the latter. The geometric constraint and electronic effect exerted by the substrate may or may not destroy the stability of an approaching magic cluster. For example, according to a calculation [8], Na_8 (a magic cluster in free space) retains its intrinsic structure after landing on the insulating NaCl(100) surface, but it spontaneously collapses on the Na(110) surface. Therefore, it is of fundamental interest to search for direct evidence of 2D magic clusters and study the cluster-surroundings interaction that needs not to be considered for magic clusters in free space. The recent interests in 2D magic clusters are also related to emerging attempts to coat surfaces with size-selected clusters [10]. Since the formation of 2D magic clusters is a plausible approach to the creation of this type of novel material, it is important to experimentally demonstrate the existence of 2D magic clusters and understand the conditions and mechanism for their formation.

In this Letter, we report the first direct observation of 2D magic clusters on the $\sqrt{3} \times \sqrt{3}R30°$ reconstructed Ga/Si(111) surface using a scanning tunneling microscope (STM) [11]. We have identified the magic numbers for these triangular clusters and observed characteristic vacancies on their surrounding $\sqrt{3} \times \sqrt{3}R30°$ adatom lattice. The vacancies are believed to be related to the preferred orientation of the clusters with respect to the substrate. These findings vividly demonstrate the interplay between the cluster and its surroundings that leads to the formation of 2D magic clusters.

Part of the reasons for choosing Ga for the study is because of its tendency to form various kinds of particular clusters in its liquid state. This unusual behavior is believed to be related to the peculiar phenomenon that Ga liquid can be supercooled to one-half of its melting temperature [12]. Although the peculiar Ga clustering phenomenon has never been studied on any substrate surface to our knowledge, adsorption of Ga on various substrates has been examined. Specifically, adsorption of Ga on the Si(111) surface has been studied extensively using various surface analytical techniques [13–15]. Deposition of $\frac{1}{3}$ monolayer (ML) ($1\,\mathrm{ML} = 7.8 \times 10^{14}\ \mathrm{Ga/cm^2}$) of Ga and subsequent annealing at ~550 °C lead to the formation of $\sqrt{3} \times \sqrt{3}R30°$ adatom surface lattice (henceforth abbreviated as adatom lattice). Recent STM studies have revealed that the position of the Ga is on the fourfold-coordinated site (T_4), rather than the threefold-coordinated hollow site (H_3), which was intuitively assigned to be the more stable bonding configuration [16,17]. Another interesting finding about this system was that higher Ga coverage (~0.8 ML) and subsequent annealing temperature at 300–500 °C resulted in the formation of hexagonally closed packed aggregates with an approximate periodicity of 2.4 nm [18]. These so called supercells were identified with the 6.3×6.3 incommensurate overlayer structure [19].

Our experiment was conducted in an ultrahigh vacuum (UHV) chamber equipped with a low energy electron diffraction (LEED) optics and a variable temperature STM (Omicrom VT-STM). The base pressure of the chamber was maintained at 8×10^{-11} Torr. Highly B-doped Si(111) substrates with resistivity of ~0.01 Ohm cm and typical terrace size of ~200 nm were used throughout the experiments. The Si substrates were cleaned by the resistive flashing in UHV until a high quality 7×7 reconstruction was observed by both LEED and STM. High purity Ga (99.999 99%) was then

 0031-9007/98/81(1)/164(4)$15.00

deposited onto the surface using an effusion cell heated by electron beam bombardment. The typical deposition rate was set at ~1 ML/min using the coverage of $\frac{1}{3}$ ML needed for the $\sqrt{3} \times \sqrt{3}R30°$ reconstruction as the relative coverage calibration. The temperature calibration was achieved by pyrometry with an estimated accuracy of ±30 °C.

We deliberately employed a two-step procedure for the sample preparation. The $\sqrt{3} \times \sqrt{3}R30°$ surface was prepared by a first deposition of $\frac{1}{3}$ ML of Ga at room temperature (25 °C) and subsequent annealing at 550 °C. Following a second deposition of ~ $\frac{1}{6}$ ML of Ga, the sample was annealed for ~10 sec at temperatures between 200 and 500 °C. The careful sample preparation enabled us to follow the behavior of adatoms after various postdeposition treatments. Most of the STM observations were carried out at room temperature except some high temperature (~ 400 °C) imaging was carried out for studying the thermal stability of the clusters.

Immediately after the second Ga deposition onto the $\sqrt{3} \times \sqrt{3}R30°$ surface, Ga droplets and vacancies, 1–2 nanometers in size, are formed simultaneously on the adatom lattice. Subsequent annealing leads to the healing of the adatom lattice with some aggregation of Ga along the step edges as well as the formation of many small clusters in the middle of terraces. Figure 1 is a typical STM image showing these clusters imbedded in the $\sqrt{3} \times \sqrt{3}R30°$ adatom lattice. The majority of these clusters are triangular and they exhibit size preference, indicating the existence of magic numbers. Based on close examinations of many atomically resolved STM images covering a total area of ~$(140\ \text{nm})^2$, a histogram for the clusters is compiled (Fig. 2). For the cluster counting, two atoms are considered to belong to the same cluster if their apparent lateral separation is less than the size of the unit cell (0.66 nm) of the adatom lattice. (Since our main concern is in clusters, we have chosen not to include monomers and dimers in Fig. 2.) The histogram clearly shows the existence of magic clusters in this system. The magic numbers are $n(n + 1)/2$, where n (2, 3, 4, or 5) is the number of atoms on each side of the cluster. Decamer ($n = 4$) is the most abundant and stable species. Its stability is further confirmed by prolonged *in situ* STM imaging at elevated temperatures. Noticeable disappearance of the decamers starts only at temperatures beyond ~350 °C, leading to the growth of much larger clusters through the Oltswald ripening process.

A detailed image of a decamer is shown in Fig. 3. It has a characteristic triangular shape with four atoms along each side. Three atoms on the corners and the one at the center occupy the original T_4 sites of the adatom lattice. Six additional atoms on the sides appear approximately on the degenerate T_4 sites that do not belong to the original adatom lattice. If we temporarily ignore the detailed positions of these additional atoms, the decamer essentially assumes a 1×1 overlayer structure on the Si(111) surface. However, under careful examination, the positions of the additional atoms appear to deviate from the exact degenerate T_4 sites. We tentatively conclude that they are located at somewhere between the degenerate T_4 and the neighboring atop sites [Fig. 4(a)]. Detailed theoretical calculations are being conducted to pinpoint the precise location of each atom in a decamer [20].

As shown in Figs. 3 and 4(a), along each side of the decamer, a Ga is missing from the adatom lattice. The characteristic vacancies suggest that intracluster attraction is stronger than the Ga-substrate interaction. The magic cluster is formed at the expense of leaving vacancies on the surrounding adatom lattice. If we ignore the

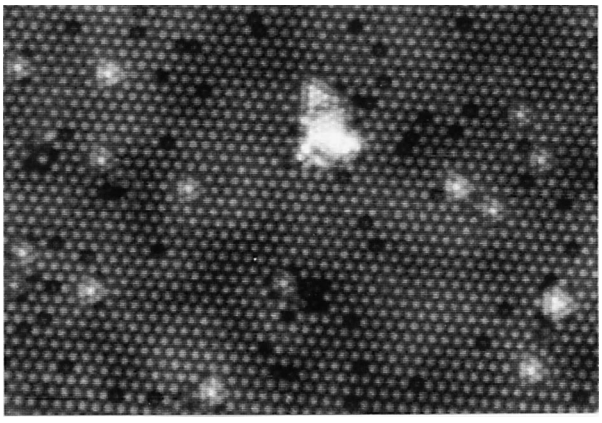

FIG. 1. STM image (size = $31 \times 21\ \text{nm}^2$) of 2D clusters on the $\sqrt{3} \times \sqrt{3}R30°$ Ga/Si(111) surface. Image was obtained with the tip bias $V_t = -1.6$ V and tunneling current $I_t = 1.8$ nA.

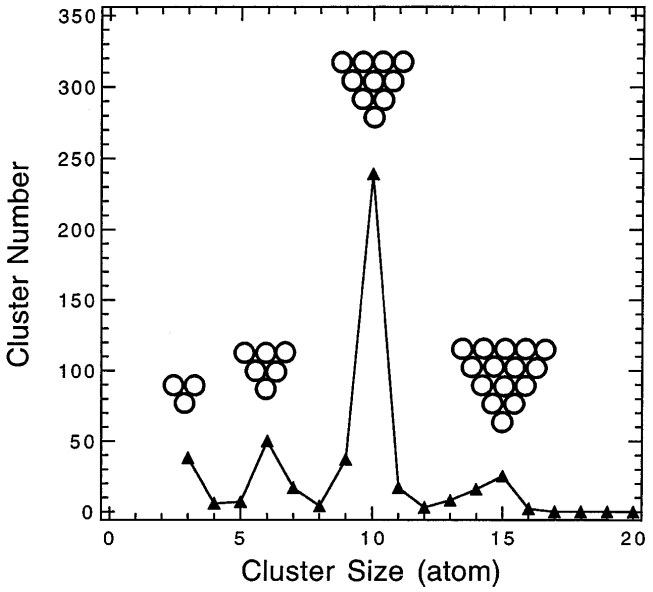

FIG. 2. Histogram of 2D clusters showing the existence of magic numbers.

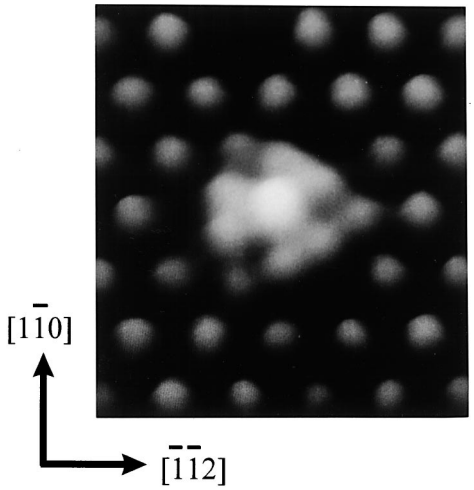

FIG. 3. STM image (size = 3.7 × 3.4 nm^2) of a decamer and the surrounding adatom lattice with characteristic pattern of vacancies. Image was obtained with $V_t = -2.5$ V and $I_t = 2.0$ nA.

effect of the substrate temporarily, and concentrate only on the adatom lattice that has sixfold symmetry, we could propose two possible structural models for the decamer as shown in Figs. 4(a) and 4(b). The main difference between the two models is in the orientation of the decamer with respect to the Si(111) substrate that has threefold symmetry. One is rotated by 60° with respect to the other. Since the orientation of the observed decamers and other 2D magic clusters are consistent with the model of Fig. 4(a) exclusively, the substrate must have a way of dictating the orientation of the clusters. Detailed examination of the models reveals that (a) has one while (b) has two Si dangling bonds associated with each vacancy on the adatom lattice. This observation suggests that the substrate could dictate the orientation of the clusters by reducing the number of Si dangling bonds in its surroundings. One could also infer that the intracluster interaction is strong enough to leave three but not six Si dangling bonds on the substrate surface. Otherwise, clusters with both types of orientations would have been observed on the surface.

Hexamers are observed exclusively in the regions with higher concentration of vacancies on the adatom lattice. Sometimes they appear on the boundary between different degenerate $\sqrt{3} \times \sqrt{3}R30°$ domains, as shown by the clusters in the middle of Fig. 5(a). The boundaries between these domains are accommodated by the formation of either $p\left(\begin{smallmatrix}2 & 0\\ 1 & 2\end{smallmatrix}\right)$ or $p\left(\begin{smallmatrix}2 & 1\\ 1 & 3\end{smallmatrix}\right)$ local adatom structures. There are one and two Si dangling bonds in each unit cell of these local structures, respectively. These local structures can also be treated as a type of ordered vacancies on the adatom lattice. Hexamers are also observed in regions with many random vacancies, as shown by the two clusters in the lower right corner of Fig. 5(a). The preferred location of hexamers seems to indicate that high concentration of vacancies, ordered or random, is essential for their formation. (Trimers are also observed exclusively in regions with high concentration of vacancies. However, because their surroundings are usually much worse defined, we decide not to discuss the details.)

The largest observed magic clusters are 15-mers [Fig. 5(b)]. However, atoms are sometimes missing from the corners of the clusters leading to the formation of 13- [Fig. 5(c)] and 14-mers. Similar to hexamers, some clusters belonging to this $n = 5$ shell exist on the boundaries between the degenerate $\sqrt{3} \times \sqrt{3}R30°$ domains [Fig. 5(b)] or in the regions with more vacancies. The characteristic vacancies along the sides of the decamer persist in the surrounding of these larger clusters. This characteristic further supports the validity of the proposed structural model for the magic clusters.

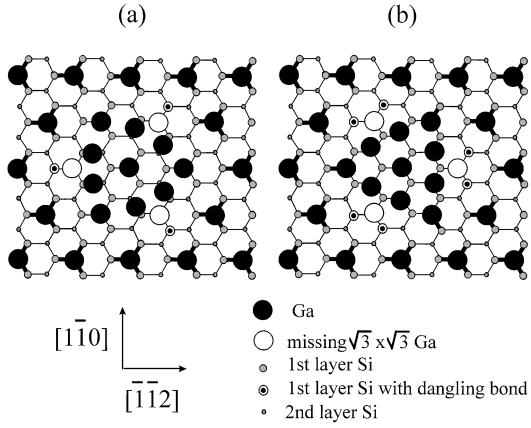

FIG. 4. Structural models for a decamer on the $\sqrt{3} \times \sqrt{3}R30°$ Ga/Si(111) surface. Model (a) is rotated by 60° with respect to (b), and each exhibits three and six Si dangling bonds in its surroundings, respectively. Orientations of the observed magic clusters are consistent with model (a) exclusively.

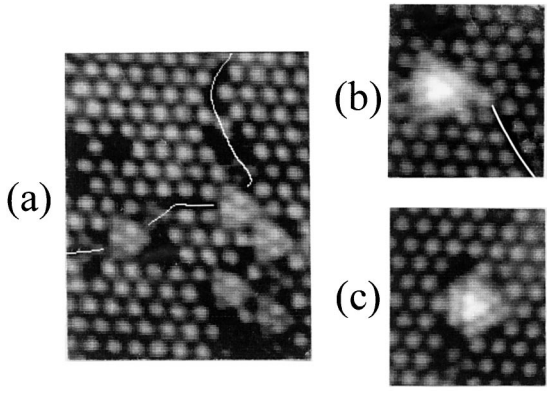

FIG. 5. STM images of (a) hexamers, (b) a 15-mer, and (c) a 13-mer. The lines on (a) and (b) indicate the boundaries between two degenerate adatom lattice domains. Images were obtained with $V_t = -2.5$ V and $I_t = 2.0$ nA, and image size = 7.2 × 8.9, 4.8 × 5.2, and 4.8 × 5.4 nm^2, respectively.

The size dispersion for the $n = 5$ clusters appears to be larger than that of the other species (Fig. 2), suggesting their lower relative stability. It could also suggest that 15-mers are created using decamers as nucleation centers, and the observed 13- and 14-mers are the remnants of the growth process.

The relative abundance among the magic clusters, especially the extraordinary abundance of the decamers, could be qualitatively understood using the model of Fig. 4(a) as a vehicle. If we ignore the substrate and adatom lattice, all the magic clusters ($n = 2$, 3, 4, or 5) exhibit closed-shell structure and threefold symmetry. These two properties could qualitatively account for the magic numbers. However, with the presence of the substrate and adatom lattice, the threefold symmetry is broken in some cases. Only decamers ($n = 4$), 28-mers ($n = 7$), 55-mers ($n = 10$), etc., preserve the threefold symmetry. The loss of threefold symmetry is most easily seen in the case of a hypothetical hexamer that exists on an ideal single $\sqrt{3} \times \sqrt{3}R30°$ domain. Such a hexamer can be created by removing a row of 4-atoms from one side of a decamer and filling the vacancy along that side at the same time. [Use the model shown in Fig. 4(a) as a template.] The resulting hexamer loses the threefold symmetry and the total number of Si dangling bonds in its surroundings becomes six, which is twice as many as that of a decamer. A similar loss of threefold symmetry and increase of surrounding dangling bonds take place when a 15-mer is constructed by adding atoms to a decamer. These examples show that, when embedded in an ideal $\sqrt{3} \times \sqrt{3}R30°$ adatom lattice, a decamer has not only higher symmetry but also a minimized number of Si dangling bonds in their surroundings. These special properties of decamers could explain their extraordinary abundance among the magic clusters. (Similar arguments based on symmetry and dangling bond minimization could also provide some clues about the fact that hexamers have never been observed on an ideal $\sqrt{3} \times \sqrt{3}R30°$ adatom lattice.)

In conclusion, we report the first direct observation of 2D magic clusters on the $\sqrt{3} \times \sqrt{3}R30°$ reconstructed Ga/Si(111) surface. In contrast to magic clusters in free space, the presence of the supporting substrate and the surrounding adatom lattice appear to play important roles in the formation of 2D magic clusters. The orientations of the clusters with respect to the substrate and the characteristic vacancies on their surrounding adatom lattice are believed to be dictated by the interplay between intracluster interaction and Ga-substrate interaction. The extraordinary abundance of magic clusters in this material system appears to be a result of their closed-shell structure and higher symmetry. However, the effect of the confined motion of electrons in a 2D island could also play a significant role in dictating the size preferences [21]. Further theoretical efforts are needed before detailed structure and formation mechanism of these interesting 2D magic clusters can be clearly understood.

We thank Dr. J. Shiao for contribution to the construction of the STM system, and Dr. J.-C. Lin, Dr. H.-C. Chang, and Dr. K.-J. Song for valuable suggestions and discussions. This work was supported partly by the National Science Council (Contract No. 87-2112-M-001-011), Taiwan, Republic of China.

*Email address: ylwang@po.iams.sinica.edu.tw

[1] W. D. Knight, K. Clemenger, W. A. de Heer, W. A. Saunders, M. Y. Chou, and M. L. Cohen, Phys. Rev. Lett. **52**, 2141 (1984).
[2] W. A. de Heer, Rev. Mod. Phys. **65**, 611 (1993).
[3] M. Brack, Rev. Mod. Phys. **65**, 677 (1993).
[4] A. W. Castleman, Jr. and K. H. Bowen, Jr., J. Phys. Chem. **100**, 12 911 (1996).
[5] M. Brack, Sci. Am. **277**, No. 6, 30 (1997).
[6] T. P. Martin, Phys. Rep. **273**, 199 (1996).
[7] G. Rosenfeld, A. F. Becker, B. Poelsema, L. K. Verheij, and G. Comsa, Phys. Rev. Lett. **69**, 917 (1992).
[8] H. Häkkinen and M. Manninen, Phys. Rev. Lett. **76**, 1599 (1996).
[9] S. K. Nayak, P. Jena, V. S. Stepanyuk, W. Hergert, and K. Wildberger, Phys. Rev. B **56**, 6952 (1997).
[10] H.-P. Cheng and U. Landman, Science **260**, 1302 (1993).
[11] G. Binnig and H. Rohrer, Rev. Mod. Phys. **59**, 615 (1987).
[12] S.-F. Tsay, Phys. Rev. B **48**, 5945 (1993); S.-F. Tsay and S. Wang, Phys. Rev. B **50**, 108 (1994).
[13] M. Zinke-Allmang and L. C. Feldman, Surf. Sci. **191**, L749 (1987).
[14] T. Thundat, S. M. Mohapatra, B. N. Dev, W. M. Gibson, and T. P. Das, J. Vac. Sci. Technol. A **6**, 681 (1988).
[15] J. R. Patel, J. Zegenhagen, P. E. Freeland, M. S. Hybertsen, J. A. Golovchenko, and D. M. Chen, J. Vac. Sci. Technol. B **7**, 894 (1989).
[16] J. Nogami, S. Park, and C. F. Quate, Surf. Sci. **203**, L631 (1988).
[17] P. Bedrossian, K. Mortensen, D. M. Chen, and J. A. Golovchenko, Nucl. Instrum. Methods Phys. Res., Sect. B **48**, 296 (1990).
[18] D. M. Chen, J. A. Golovchenko, P. Bedrossian, and K. Mortensen, Phys. Rev. Lett. **61**, 2867 (1988).
[19] M. Otsuka and T. Ichikawa, Jpn. J. Appl. Phys. **24**, 1103 (1985).
[20] S.-F. Tsay and M. H. Tsai (private communication).
[21] K. Jin, G. D. Mahan, H. Metiu, and Z. Zhang, Phys. Rev. Lett. **80**, 1026 (1998).